Journal of Advanced Research in Applied Sciences and Engineering Technology

Journal homepage:
https://semarakilmu.com.my/journals/index.php/applied_sciences_eng_tech/index
ISSN: 2462-1943

Exploring the Systematics of Cluster Decay Half-Lives in Heavy Actinides Within the Range $234 \leq A \leq 252$

Joshua Tolulope Majekodunmi[1,*], Khairul Anwar Mohamad Khazali[1], Mrutunjaya Bhuyan[2], Nooraihan Abdullah[1], Raj Kumar[3], Wasiu Akanni Yahya[4], Isaiah Ochala[5]

[1] Institute of Engineering Mathematics, Universiti Malaysia Perlis (UniMAP), 02600 Arau, Perlis, Malaysia
[2] Center for Theoretical and Computational Physics, Department of Physics, Faculty of Science, University of Malaya, 50603 Kuala Lumpur, Malaysia
[3] School of Physics and Materials Science, Thapar Institute of Engineering and Technology, Patiala, Punjab 147004, India
[4] Department of Physics and Materials Science, Kwara State University, Malete, P.M.B. 1530, Ilorin, Kwara State, Nigeria
[5] Physics Department, Prince Abubakar Audu University, Anyigba, Nigeria

ARTICLE INFO

Article history:
Received 4 November 2023
Received in revised form 17 January 2024
Accepted 11 July 2024
Available online 25 July 2024

Keywords:
Relativistic mean-field; Cluster decay; Preformed cluster model; Half-lives; Shell effects; Driving potential; Preformation probability

ABSTRACT

This study explores the cluster decay half-lives in both experimentally measured and undetected radioactive nuclei within the mass number range $234 \leq A \leq 252$. The investigation employs the recently proposed preformation probability (P_0) formula, focusing on the systematic behaviours governing cluster emissions. Emphasis is placed on the contribution of the Q-value during both preformation and decay processes. Experimental binding energy data are used to estimate Q-values, and the cluster penetration process is discussed using the M3Y and R3Y nuclear potentials. The interaction potential between the cluster and the daughter nucleus is obtained by folding the relativistic mean-field (RMF) densities with R3Y NN potential using the NL3* parameter set and compared with the phenomenological M3Y NN potential. The penetration probabilities are calculated from the WKB approximation. The P_0 formula is found to be a useful tool for understanding cluster radioactivity in heavy actinides. The result provides valuable insights into the systematics of cluster decay half-lives, highlighting the influence of neutron magic shell closures and interaction potentials on different cluster decay properties.

1. Introduction

In a groundbreaking experiment conducted by Rose and Jones in 1984 [1], a novel form of nuclear decay was identified. Amidst a substantial background of α-decay generated by the parent nucleus ^{223}Ra, a limited number of occurrences resulting in ^{14}C were detected. Subsequently, this discovery has sparked a significant amount of both experimental and theoretical endeavours aimed at understanding the factors governing cluster emissions from these heavy nuclei [2-4]. As a result, approximately 30 additional radioactive decay processes, encompassing a spectrum of clusters

* *Corresponding author.*
E-mail address: majekjoe1@gmail.com

https://doi.org/10.37934/araset.49.1.183193

ranging from ^{14}C - ^{34}Si, have been identified [5]. The concept of Cluster Radioactivity (CR) is often explained within the framework of the Gamow model of α-decays which assumes that a pre-existing cluster composed of multiple nucleons tunnelling a barrier established by the nuclear and Coulomb potentials [6,7]. The exponential reliance of tunnelling probability on barrier parameters results in a modified Geiger-Nuttall law [8,9], which establishes a connection between CR half-lives and the Q-value of the reaction.

Cluster decay models are typically classified into two main categories i.e. the fission-like models and the α-decay-like models. The fission-like models operate on the premise that cluster formation occurs as the parent nucleus continuously experiences deformation while overcoming the interaction barrier. An example of such a model is the Analytic Super Asymmetric Fission Model (ASAFM) proposed by Poenaru *et al.,* [10,11]. In contrast, the latter category of models e.g. the preformed cluster-decay model (PCM) [12,13] operates on the premise of natural cluster birth, implying that the clusters are assumed to already exist (preformed) within the parent nuclei.

Numerous studies have been dedicated to exploring the preformation probability (P_0) with commendable predictive capabilities. Nevertheless, there is an intriguing interest in formulating a unified formula for P_0 whose applicability extends across the entire nuclear chart. Furthermore, instead of adjusting such formulas with arbitrary constants, it is pertinent to elucidate their physical significance in relation to the kinematics and fundamental principles governing cluster emission. To address this problem, we have recently proposed a new formula for P_0 [17] that captures the influential parameters on cluster radioactivity. Apart from the P_0, another complexity within the many-body problem is the variability of the nuclear potential. Here, the phenomenological M3Y NN potential is fitted to the G-matrix element based on the Reid-Elliott soft-core NN interaction [18] in an oscillator basis. An analogous potential titled "R3Y" have been microscopically derived from the relativistic mean-field (RMF) Lagrangian and successfully applied to the cluster radioactive decays [4,19,20].

This work revisits and extends previous study [21], which had only considered experimentally verified cluster decays, to further investigate the decay properties of undetected (predicted) radioactive systems. The present study delves into the cluster decay half-lives of radioactive nuclei within the mass range $234 \leq A \leq 252$ using the M3Y and R3Y nucleon-nucleon (NN) potentials. It employs the recently proposed P_0 formula to investigate the systematic behaviours governing cluster emissions. Emphasis is placed on the contribution of the Q-value during both preformation and decay processes. The study also considers the impact of neutron magic shell closures on cluster decay characteristics. This study also theoretically analyses certain parameters such as the driving potential, shell effects, penetration probability (P) via the WKB approximation and the cluster decay half-lives using the PCM.

In Section II, we provide a concise overview of the theoretical framework, encompassing the non-linear RMF Lagrangian, the double-folding methodology applied to both R3Y and M3Y potentials, the PCM, as well as our recently formulated P_0 formula and its components. Section III delves into the discussion of the results obtained. Lastly, in Section IV, we present the conclusion and a summary of the key findings in this study.

2. Theoretical Formalism

2.1 The Relativistic Mean-Field (RMF)

The construction of the traditional RMF model involves the interplay between the nucleon and three mesons i.e. the isoscalar-scalar field σ, the isoscalar-vector field ω, and the isovector-vector field ρ. The RMF Lagrangian density is of the form [4,17-24]

$$\begin{aligned} L = {} & \bar{\psi}\left\{ i\gamma^{\mu}\partial_{\mu} - M \right\}\psi + \frac{1}{2}\partial^{\mu}\sigma\partial_{\mu}\sigma - \frac{1}{2}m^{2}{}_{\sigma}\sigma^{2} - \frac{1}{3}g_{2}\sigma^{3} - \frac{1}{4}g_{3}\sigma^{4} - g_{s}\bar{\psi}\psi\sigma \\ & - \frac{1}{4}\Omega^{\mu\nu}\Omega_{\mu\nu} + \frac{1}{2}m_{\omega}^{2}\omega^{\mu}\omega_{\mu} - g_{\omega}\bar{\psi}\gamma^{\mu}\psi\omega_{\mu} - \frac{1}{4}\vec{B}^{\mu\nu}\vec{B}_{\mu\nu} + \frac{1}{2}m_{\rho}^{2}\rho^{\mu}\vec{\rho}_{\mu} \\ & - g_{\rho}\bar{\psi}\gamma^{\mu}\vec{\tau}\psi.\vec{\rho}^{\mu} - \frac{1}{4}F^{\mu\nu}F_{\mu\nu} - e\bar{\psi}\gamma^{\mu}\frac{\left(1-\tau_{3}\right)}{2}\psi A_{\mu}. \end{aligned} \tag{1}$$

The coupling constants for the non-linear terms are denoted as g_2, g_3, and $e^2/4\pi$. The third component of the isospin is represented by τ_{3i}. Nucleons have a mass denoted as M, while the masses of the σ, ω and ρ mesons are denoted as m_σ, m_ω, and m_ρ respectively. The fields corresponding to these mesons are ω^{μ}, ρ_{μ} and A_{μ}. It is important to highlight that the contribution of the π-meson is neglected in Eq. (1) when calculating the mean field due to its pseudo-scalar nature [24,25]. A comprehensive description of the field tensors is given in [26] and the references therein. These field tensors are treated as classical fields using the Dirac equation for the nucleons and the Klein-Gordon equations for the mesons. These equations are self-consistently solved employing the NL3* parameter set. In the limit of one-meson exchange within a heavy and stationary baryonic medium, the microscopic R3Y NN potential is derived as:

$$V_{eff}^{R3Y}(r) = \frac{g_{\omega}^{2}}{4\pi}\frac{e^{-m_{\omega}r}}{r} + \frac{g_{\rho}^{2}}{4\pi}\frac{e^{-m_{\rho}r}}{r} - \frac{g_{\sigma}^{2}}{4\pi}\frac{e^{-m_{\sigma}r}}{r} + \frac{g_{2}^{2}}{4\pi}re^{-2m_{\sigma}r} + \frac{g_{3}^{2}}{4\pi}\frac{e^{-3m_{\sigma}r}}{r} + J_{00}(E)\delta(r), \tag{2}$$

where $J_{00}(E)\delta(r)$ stands for the pseudopotential describing the zero-range exchange effect. Similarly, the M3Y NN potential is expressed as

$$V_{eff}^{M3Y}(r) = 7999\frac{e^{-4r}}{4r} - 2134\frac{e^{-2.5r}}{2.5r} + J_{00}(E)\delta(r). \tag{3}$$

The nuclear interaction potential V_n (R) between the emitted cluster and the daughter nucleus is determined by integrating the NN potentials over the nuclear densities, using the widely known double folding approach [18]

$$\mathrm{V_n}\left(\vec{R}\right) = \int \rho_{c}(r_{c})\rho_{d}(r_{d})V_{eff}\left(\left|r_{c} - r_{d} + R\right| \equiv r\right)d^{3}r_{c}d^{3}r_{d}. \tag{4}$$

The densities of the emitted clusters and the daughter nuclei are denoted by ρ_c and ρ_d respectively. These nuclear potentials combine with the Coulomb potential to obtain the total interaction potential which is employed to estimate the decay half-lives within the PCM [27].

2.2 The Preformed Cluster-Decay Model (PCM)

Within the PCM, the decay constant and half-life $T_{1/2}$ for cluster decays are expressed as

$$\lambda = \nu_0 P_0 P, \qquad T_{1/2} = \frac{In2}{\lambda}, \tag{5}$$

P represents the penetration probability, mathematically expressed as

$$P = P_a P_b. \tag{6}$$

P_a and P_b denote the penetration probabilities from the initial classical turning point R_a to a de-excitation point R_i where it penetrates again and terminates at the final turning point in the cluster-decay process (not graphically shown here. Elaborate details are given in [4,20]). Following the WKB approximation, P_a and P_b can be simply expressed as

$$P_a = \exp\left[-\frac{2}{h}\int_{Ra}^{Ri} \left\{2\mu[V(R) - V(R_i)]\right\}^{1/2} dR \right] \tag{7}$$

and

$$P_b = \exp\left[-\frac{2}{h}\int_{R_i}^{R_b} \left\{2\mu[V(R_i) - Q]\right\}^{1/2} dR \right], \tag{8}$$

where μ denotes the reduced mass given by $\mu = A_d A_c / (A_d + A_c)$.

Instead of employing the conventional cluster-mass-dependent P_0 formula introduced by Blendowske and Walliser [14], our approach focuses on a comprehensive analysis of the interrelationships among various theoretically established factors affecting cluster preformation. These factors include the cluster mass A_c [19], mass and charge asymmetries $\eta_A = (A_d - A_c)/(A_d + A_c)$ and $\eta_Z = (Z_d - Z_c)/(Z_d + Z_c)$, considering that experimental observations confirm the possibility of emission of the same cluster from different parent nuclei as well as the emission of different clusters from the same parent nucleus [5,28]. Additionally, we consider the relative separation between the centres of the fragments, denoted as $r_B = 1.2(A_d^{1/3} + A_c^{1/3})$ [29], and the Q-value [30]. As a result, we have recently proposed a novel P_0 formula [17].

$$\log P_0 = -\frac{aA_c\eta_A}{r_B} - Z_c\eta_Z + bQ + c, \tag{9}$$

where a, b and c are the fitting parameters whose values are given in Table 1. These values have been found to be consistent in reproducing the experimentally measured data in this region of study [17,21,31].

Table 1
Nonlinear least-square fitting parameters a, b and c for the preformation formula in Eq. (9) for established experimentally favoured cluster decays

System	a	b	c
e-e	17.67	0.114	8.00
	11.98¶	0.037¶	3.56¶
O-A	16.12	0.119	0.88†
	16.12	0.119	4.02§

¶Valid for systems yielding the double magic ^{208}Pb daughter nucleus
†Parameter c appears lower for systems having daughters with non-magic neutron numbers ($N_d \leq 126$).
§Systems having daughters with a magic neutron (or neighbours) require a higher value of parameter c ($126 \leq N_d \leq 128$).

Moreover, the third term on the right side of Eq. (9) introduces a novel perspective for investigating the implications of decay energy. In essence, the term bQ provides a quantifiable representation of the "energy contributed during cluster formation." Consequently, for the first time, we present the Q-value in the context of its allocation and utilization in cluster emission as

$$Q = \underbrace{bQ}_{\substack{\text{energy contributed in} \\ \text{cluster formation}}} + \underbrace{\kappa\sqrt{Q}}_{\substack{\text{energy} \\ \text{contributed in} \\ \text{cluster emission}}} + \underbrace{E_d}_{\substack{\text{recoil} \\ \text{energy of} \\ \text{daughter nucleus}}} . \tag{10}$$

Here, $\kappa\sqrt{Q}$ denotes the energy contributed during cluster emission. Building on the research conducted by Gupta *et al.,* [19], we express the kinetic energy of the emitted cluster as:

$$E_c = \frac{A_d}{A} Q = bQ + \kappa\sqrt{Q}. \tag{11}$$

These parameters are further analysed and concisely discussed in the subsequent section.

3. Results

The cluster decay half-lives of radioactive nuclei with mass numbers within the range $234 \leq A \leq 252$ are examined to explore the systematics governing their respective emissions using the recently proposed P_0 formula [17]. We reiterate that this formula does not only accurately capture the influential parameters of cluster radioactivity but also theoretically suggests how the Q-value is expended within the decay process. Here, the Q-values are estimated from the experimental binding energy data [32]. The emitted clusters undergo a three-step penetration process as shown in the profile of the total interaction potentials elaborately described in [13,31]. The M3Y and R3Y NN potentials display similar pattern but exhibit different barrier characteristics which often require a modification of the entrance channel via the neck-length parameter ΔR [20]. We have earlier established that the most suitable ΔR value for the phenomenologically fitted M3Y NN potential is 0.5 fm [24] while the relativistic R3Y NN potential conveniently accommodates 1.0 fm [4] in cluster decays.

3.1 The Driving Potential (D_{pot})

Table 2 depicts the variation in the driving potential of different experimentally verified heavy actinides yielding daughters at (or around) the neutron shell closure N_d = 126, using the M3Y and the R3Y NN potentials. The systematics of three different experimentally validated possibilities are considered. First, the emission of clusters of varied masses from different parent nuclei, yielding similar daughter nuclei. A vivid example is ^{238}Pu → ^{32}Si + ^{206}Hg and ^{240}Pu → ^{34}Si + ^{206}Hg. It is worth noting that the predicted magnitudes of the M3Y are all time higher than those of the R3Y as a result of the aforementioned difference in their respective barrier properties. As such, a concerted effort is primarily made to explore the similar qualitative description of the physics in the profiles of the reaction systems. It is evident that the massive cluster yields a lower driving potential, provided that none of the reaction systems yields a magic daughter nucleus. Secondly, we consider a situation where different parent nuclei emit clusters of the same mass e. g. ^{240}Pu → ^{34}Si + ^{206}Hg and ^{241}Am → ^{34}Si + ^{207}Tl. In this case, the massive parent nucleus also yields the least driving potential, and a much lower value could be obtained when the reaction system yields a magic daughter nucleus such as ^{242}Cm → ^{34}Si + ^{208}Pb.

Table 2
The driving potential $D_{pot} = VR_a - Q$ calculated from both M3Y and R3Y predictions. The Q-values are estimated from [28] the experimental binding energies to ensure accuracy

Parent nuclei	Emitted Cluster	Daughter nuclei	$D_{pot} = VR_a - Q$ (MeV)	
			M3Y	R3Y
^{238}Pu	^{32}Si	^{206}Hg	28.531	7.298
^{240}Pu	^{34}Si	^{206}Hg	27.781	5.844
^{241}Am	^{34}Si	^{207}Tl	26.427	4.427
^{242}Cm	^{34}Si	^{208}Pb	16.605	1.059
^{252}Cf	^{46}Ar	^{206}Hg	24.698	0.440
^{252}Cf	^{48}Ca	^{204}Pt	28.494	5.615
^{252}Cf	^{50}Ca	^{202}Pt	26.244	0.756

The third case highlights the emission of different fragments (emitted clusters and daughter nuclei) from the same parent nuclei. Here, we observe that two main factors can influence the driving potential i.e. the proximity of the neutron number of the daughter nuclei to the magic number e.g. ^{252}Pu → ^{46}Ar + ^{206}Hg and ^{252}Pu → ^{48}Ca + ^{204}Pt. Although, in both systems N_d = 126, it is evident that the massive cluster ^{48}Ca yields a D_{pot} value. Similarly, the nearness of the neutron number of the emitted cluster to the magic number e.g ^{252}Pu → ^{50}Ca + ^{202}Pt having N_d = 124 yields a relatively lower D_{pot} value than ^{252}Pu → ^{48}Ca + ^{204}Pt but higher than ^{252}Pu → ^{46}Ar + ^{206}Hg since the emitted cluster is a magic nucleus with A_c = 50. This affirms the important role of closed shells in the cluster-decay process. Typically, the driving potential is susceptible to both the selected interaction potential and the characteristics of the decaying parent nucleus, along with the resulting decay fragments (which include clusters and the daughter nucleus). Besides, the cold valleys in the computed driving potentials of binary fragmentations often reveal the most probable decay modes of a reaction system [33].

3.2 The Nuclear Potential

The impact of the neutron magic shell closure is further revealed in the profile of the nuclear potential V_n as portrayed in Figure 1. Apart from the magnitude difference in the M3Y and R3Y predictions, it is salient to note that the neutron number of all the ^{34}Si cluster emitting systems in the figure is N_d = 126. In both NN potentials, the uniform observation is that the magnitude of V_n for the system yielding ^{206}Hg (dark yellow dashes and solid lines) nearly overlaps with those of ^{207}Tl while that of ^{208}Pb maintains the same profile but distends with lower value due to its double magic nature. The relativistic R3Y NN potential clearly captures the trend in their respective magnitudes. The nuclear potentials are used as inputs within the WKB approximation to obtain the penetration probabilities.

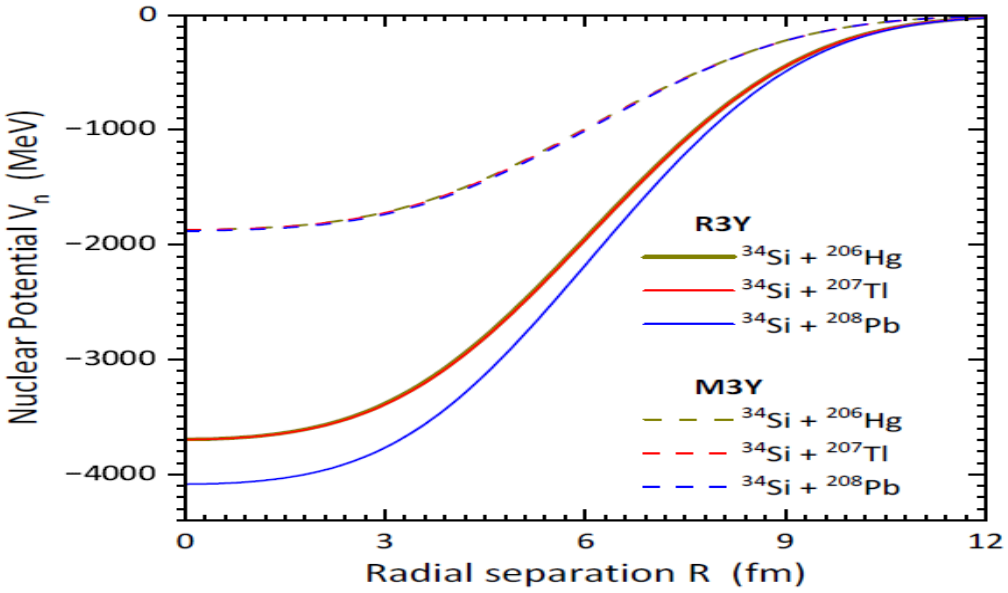

Fig. 1. Nuclear potentials (Vn) calculated from the M3Y and R3Y NN potentials for different systems emitting 34Si -cluster

3.3 The Penetration Probabilities

Figure 2 illustrates the variation of the penetration probabilities (in logarithmic scale) for different systems emitting ^{34}Si clusters with daughter nuclei at N_d = 126 and in its neighbourhood. It is clear that the penetration probabilities decrease with respect to the increasing mass of the parent nuclei. The estimated $-\log_{10} P$ for the M3Y (dash lines with blue open circles) and R3Y (solid line with black squares) potentials are quite close in magnitude except for ^{242}Cm → ^{34}Si + ^{208}Pb where a minimum is formed at the double magic shell closure ^{208}Pb-daughter nucleus. The penetration probability is an indispensable parameter for calculating the decay half-lives.

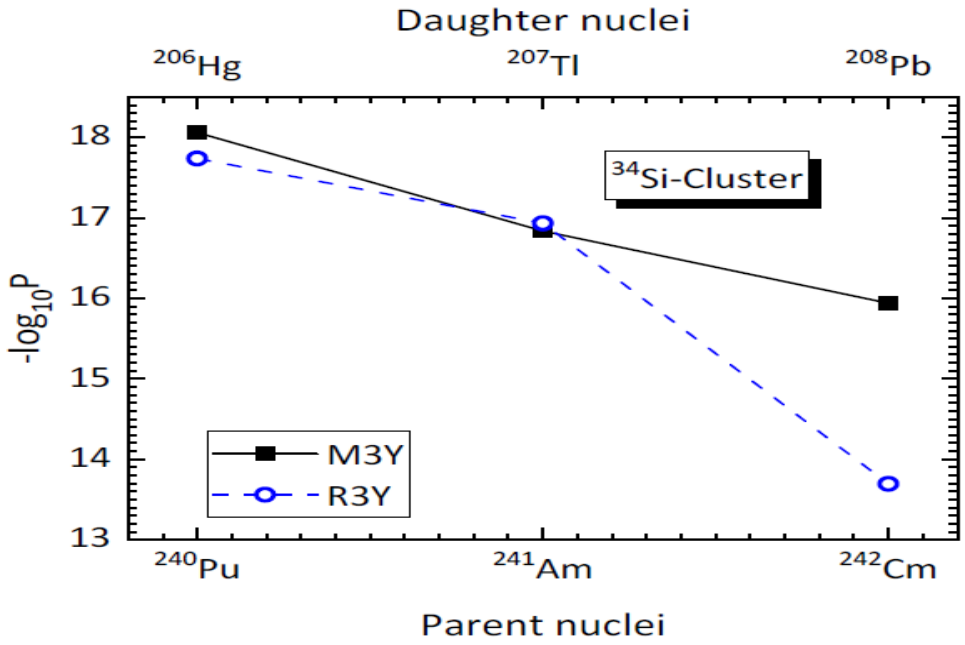

Fig. 2. The profiles of the penetration probability P (in logarithmic scale) for ^{14}C emission from different actinides

3.4 Cluster Decay Half-Lives

While experimental evidence supports cluster decay as a prominent decay mechanism in the heavier trans-lead region, a comprehensive theory that encompasses all facets of cluster decay has not yet been developed. Thus, a conscious effort is made to estimate the cluster decay half-lives of some undetected radioactive systems as shown in the upper panel of Table 3. It is worth mentioning that the calculated half-life values in column 7 are solely based on the R3Y NN potential and are found to agree closely with the predictions in [27] and those of universal decay law (UDL) [34]. This inference does not only assert the reliability of the aforementioned models but also provides a potential guide for future experimental endeavours.

Although the precise half-lives of most of the examined reaction systems are not experimentally known, the PCM predicted values are in good agreement with the experimentally measured lower limits and the known physics in cluster radioactivity. As discussed earlier, the quantitative difference in the M3Y and R3Y is ignored in this analysis while deliberate attention is given to the unanimous qualitative description of both NN potentials. The lower panel of Table 3 unequivocally shows the presence of a minima in $-\log_{10} P$ and $\log_{10} T_{1/2}$ for the double magic daughter ^{208}Pb. In principle, the shortest value of the half-life is obtained when the daughter nucleus has a magic number of neutrons (N_d = 126) and/or protons (Z_d = 82). In other words, the dominance of double magic structure in heavy fragment is shown to reveal the strong influence of shell effects on cluster radioactivity as earlier opined by Warda *et al.,* [35].

Table 3
The decay half-lives and preformation characteristics of different clusters, which have been experimentally observed yielding N_d = 126 or a daughter nucleus in its neighbourhood. The Q-value, bQ, $\kappa\sqrt{Q}$, E_c and E_d are measured in MeV

Parent	Cluster	Daughter	Q-value	$\log_{10} T_{1/2}$			P_0	bQ	$\kappa\sqrt{Q}$	E_c	E_d
nuclei		nuclei		[27]	UDL	R3Y	Eq. (9)				
^{234}Pu	^{24}Ne	^{210}Po	62.25	22.17	23.38	22.13	2.59×10^{-25}	7.11	48.76	55.87	6.39
^{234}Pu	^{28}Mg	^{206}Pb	79.15	17.62	21.81	21.33	1.06×10^{-27}	9.05	60.64	69.68	9.47
^{237}Pu	^{29}Mg	^{208}Pb	77.44	22.36	25.52	24.13	4.37×10^{-29}	9.25	58.72	67.97	9.48
^{238}Pu	^{28}Mg	^{210}Pb	75.91	23.12	28.80	24.37	4.17×10^{-28}	8.67	58.31	66.98	8.93
				Expt.	M3Y	R3Y					
^{238}Pu	^{32}Si	^{206}Hg	91.19	25.27	25.17	24.88	4.40×10^{-30}	10.42	68.51	78.93	12.26
^{240}Pu	^{34}Si	^{206}Hg	91.06	>25.52	26.55	26.75	2.15×10^{-31}	10.41	67.76	78.16	12.90
^{241}Am	^{34}Si	^{207}Tl	93.96	>22.71	24.89	25.71	3.68×10^{-31}	11.22	69.48	80.70	13.26
^{242}Cm	^{34}Si	^{208}Pb	96.51	23.24	23.70	25.46	3.80×10^{-30}	3.57	79.38	82.95	13.56
^{252}Cf	^{46}Ar	^{206}Hg	126.75	>15.89	25.73	28.14	5.77×10^{-35}	14.48	89.13	103.61	23.14
^{252}Cf	^{48}Ca	^{204}Pt	137.97	>15.89	26.58	25.81	9.13×10^{-35}	15.77	95.92	111.69	26.28
^{252}Cf	^{50}Ca	^{202}Pt	138.32	>15.89	26.28	28.05	2.89×10^{-35}	15.81	95.07	110.87	27.44

A careful inspection of column 8 of Table 3 shows that among clusters of the same size like ^{34}Si, the preformation at double shell closures will be higher e.g. $P_0 = 3.80\times10^{-30}$ (This conjecture is also true for the examined undetected cluster decays). Thus, unlike the expression of Blendoskwe and Walliser [14], ($P_0^{BW} = S^{\frac{A_c-1}{3}}$, $S_{even} = 0.0063$ which is valid for $A_c \leq 28$ and whose result yields a constant value for different systems emitting the same cluster), the shell effect is prominent with the new P_0 expression in Eq. (9). The analysis of the break-up or contribution of the Q-value at this point (where the shell effect is mostly prominent) reveals that bQ will be least since the parameter b captures the odd-even staggering effect which is not feasible in ^{242}Cm → ^{34}Si + ^{208}Pb (being an even-even system) and thus $bQ = 3.57$ MeV. This conjecture increases the tunnelling factor κ and thus parameter $\kappa\sqrt{Q} = 79.38$ MeV and similar increases are noticed in $E_c = bQ + \kappa\sqrt{Q}$ and the recoil energy E_d as shown in columns 9 - 12**.** The notable inference that can be drawn here is that the shell effects is central to structural properties of a decaying nucleus.

4. Conclusions

The cluster decay mechanism is systematically studied within the mass range $234 \leq A \leq 252$. The relativistic mean-field (RMF) formalism is employed using the NL3* parameter set. By taking the assumption of a pre-formed cluster, our recently proposed P_0 formula is employed. Furthermore, in order to validate the applicability of the formula, the widely known M3Y and the microscopic-based R3Y NN potentials are used for the analysis. Despite variations in their respective barrier properties, our findings demonstrate that the incorporation of the new P_0 formula results in calculated half-lives that align well with the experimental data. The driving potential and other examined parameters are found to be highly influenced by the proximity of daughter nuclei to magic number. In other words, neutron magic shell closures play a significant role in determining cluster decay properties, highlighting the influence of shell effects on cluster radioactivity. This conjecture is also found to be true for the examined predicted radioactive systems.

The influence of nuclear deformations in both the decaying nucleus and the decay fragments is recognized as a considerable factor in cluster decays. Nevertheless, this effect may be relatively less pronounced during the actual cluster formation but could become more significant as the process progresses towards the scission point. This will be the direction for our future work.

Acknowledgement
The authors would like to acknowledge the support from the Fundamental Research Grant Scheme (FRGS) under the grant number FRGS/1/2019/STG02/UNIMAP/02/2 from the Ministry of Education Malaysia stipulated with the Institute of Engineering Mathematics (IMK)- UniMAP as the beholder, Science and Engineering Research Board (SERB), File No. CRG/2021/001229, FOSTECT Project Code: FOSTECT.2019B.04 and FAPESP Project Nos. 2017/05660-0.

References

[1] Rose, H. J., and G. A. Jones. "A new kind of natural radioactivity." *Nature* 307, no. 5948 (1984): 245-247. https://doi.org/10.1038/307245a0
[2] Poenaru, Dorin N., M. Ivascu, A. Sandulescu, and W. Greiner. "Spontaneous emission of heavy clusters." *Journal of Physics G: Nuclear Physics* 10, no. 8 (1984): L183. https://doi.org/10.1088/0305-4616/10/8/004
[3] Zhang, H. F., J. M. Dong, Guy Royer, W. Zuo, and J. Q. Li. "Preformation of clusters in heavy nuclei and cluster radioactivity." *Physical Review C* 80, no. 3 (2009): 037307. https://doi.org/10.1103/PhysRevC.80.037307
[4] Majekodunmi, Joshua T., M. Bhuyan, D. Jain, K. Anwar, N. Abdullah, and Raj Kumar. "Cluster decay half-lives of Ba 112–122 isotopes from the ground state and intrinsic excited state using the relativistic mean-field formalism within the preformed-cluster-decay model." *Physical Review C* 105, no. 4 (2022): 044617. https://doi.org/10.1103/PhysRevC.105.044617
[5] Bonetti, Roberto, and Alessandra Guglielmetti. "Cluster radioactivity: an overview after twenty years." *Romanian reports in Physics* 59, no. 2 (2007): 301.
[6] Poenaru, D. N., R. A. Gherghescu, and W. Greiner. "Single universal curve for cluster radioactivities and α decay." *Physical Review C* 83, no. 1 (2011): 014601. https://doi.org/10.1103/PhysRevC.83.014601
[7] Tavares, O. A. P., and E. L. Medeiros. "A simple description of cluster radioactivity." *Physica Scripta* 86, no. 1 (2012): 015201. https://doi.org/10.1088/0031-8949/86/01/015201
[8] Qi, Chong, F. R. Xu, Roberto J. Liotta, and Ramon Wyss. "Universal decay law in charged-particle emission and exotic cluster radioactivity." *Physical review letters* 103, no. 7 (2009): 072501. https://doi.org/10.1103/PhysRevLett.103.072501
[9] Ni, Dongdong, Zhongzhou Ren, Tiekuang Dong, and Chang Xu. "Unified formula of half-lives for α decay and cluster radioactivity." *Physical Review C* 78, no. 4 (2008): 044310. https://doi.org/10.1103/PhysRevC.78.044310
[10] Poenaru, Dorin N., M. Ivaşcu, A. Sndulescu, and Walter Greiner. "Atomic nuclei decay modes by spontaneous emission of heavy ions." *Physical Review C* 32, no. 2 (1985): 572. https://doi.org/10.1103/PhysRevC.32.572
[11] Poenaru, D. N., W. Greiner, K. Depta, M. Ivascu, D. Mazilu, and A. Sandulescu. "Calculated half-lives and kinetic energies for spontaneous emission of heavy ions from nuclei." *Atomic Data and Nuclear Data Tables* 34, no. 3 (1986): 423-538. https://doi.org/10.1016/0092-640X(86)90013-6
[12] Singh, Birbikram, S. K. Patra, and Raj K. Gupta. "Importance of preformation probability in cluster radioactive-decays using relativistic mean field theory within the preformed cluster model." *International Journal of Modern Physics E* 20, no. 04 (2011): 1003-1007. https://doi.org/10.1142/S0218301311019143
[13] Majekodunmi, Joshua T., Theeb YT Alsultan, K. Anwar, Nujud Badawi, D. Jain, Raj Kumar, and M. Bhuyan. "The α-particle clustering and half-lives of the newly discovered 207,208 Th decay chains within relativistic-Hartree-Bogoliubov approach." *Nuclear Physics A* 1034 (2023): 122652. https://doi.org/10.1016/j.nuclphysa.2023.122652
[14] Blendowske, R., and H. Walliser. "Systematics of cluster-radioactivity-decay constants as suggested by microscopic calculations." *Physical review letters* 61, no. 17 (1988): 1930. https://doi.org/10.1103/PhysRevLett.61.1930
[15] Santhosh, K. P., and Tinu Ann Jose. "Theoretical investigation on double-α decay from radioactive nuclei." *Physical Review C* 104, no. 6 (2021): 064604. https://doi.org/10.1103/PhysRevC.104.064604
[16] Ni, Dongdong, and Zhongzhou Ren. "Half-lives and cluster preformation factors for various cluster emissions in trans-lead nuclei." *Physical Review C* 82, no. 2 (2010): 024311. https://doi.org/10.1103/PhysRevC.82.024311
[17] Majekodunmi, Joshua T., Raj Kumar, and M. Bhuyan. "Quest for a Universal Cluster Preformation Formula: A new paradigm for estimating the cluster formation energy." Europhysics Letters 143, (2023): 24001. https://doi.org/10.1209/0295-5075/ace475

[18] Satchler, George Raymond, and W. Gary Love. "Folding model potentials from realistic interactions for heavy-ion scattering." *Physics Reports* 55, no. 3 (1979): 183-254. https://doi.org/10.1016/0370-1573(79)90081-4
[19] Singh, BirBikram, S. K. Patra, and Raj K. Gupta. "Cluster radioactive decay within the preformed cluster model using relativistic mean-field theory densities." *Physical Review C* 82, no. 1 (2010): 014607. https://doi.org/10.1103/PhysRevC.82.014607
[20] Majekodunmi, Joshua T., Shilpa Rana, Nishu Jain, K. Anwar, N. Abdullah, Raj Kumar, and M. Bhuyan. "Relativistic R3Y Nucleon–Nucleon Potential: Decay Characteristics of 124 Ba Isotope Within the Preformed Cluster Decay Approach." In *Intelligent Systems: Proceedings of ICMIB 2021*, pp. 135-142. Singapore: Springer Nature Singapore, 2022. https://doi.org/10.1007/978-981-19-0901-6_13
[21] Majekodunmi, Joshua T., M. Bhuyan, K. Anwar, D. Jain, and R. Kumar. "Cluster decay dynamics of actinides yielding non-Pb-daughter within relativistic mean field formalism." The European Physical Journal A, 60(5), (2024): 101. https://doi.org/10.1140/epja/s10050-024-01324-4
[22] Ring, Peter. "Relativistic mean field theory in finite nuclei." *Progress in Particle and Nuclear Physics* 37 (1996): 193-263. https://doi.org/10.1016/0146-6410(96)00054-3
[23] Das, Monalisa, M. Bhuyan, Joshua T. Majekodunmi, N. Biswal, and R. N. Panda. "Structure and decay chain of fermium isotopes using relativistic mean-field approach." *Modern Physics Letters A* 37, no. 21 (2022): 2250133. https://doi.org/10.1142/S0217732322501334
[24] Das, Monalisa, J. T. Majekodunmi, N. Biswal, R. N. Panda, and M. Bhuyan. "Correlation between the nuclear structure and reaction dynamics of Ar-isotopes as projectile using the relativistic mean-field approach." *Nuclear Physics A* (2023): 122703. https://doi.org/10.1016/j.nuclphysa.2023.122703
[25] Serot, Brian D., and John Dirk Walecka. "Relativistic nuclear many-body theory." *Recent Progress in Many-Body Theories: Volume 3* (1992): 49-92. https://doi.org/10.1007/978-1-4615-3466-2_5
[26] Singh, Ajeet, A. Shukla, and M. K. Gaidarov. "Cluster decay half-lives in trans-tin and transition metal region using RMF theory." *Journal of Physics G: Nuclear and Particle Physics* 49, no. 2 (2021): 025101. https://doi.org/10.1088/1361-6471/ac3c4e
[27] Kumar, Raj. "Cluster radioactivity using various versions of nuclear proximity potentials." *Physical Review C* 86, no. 4 (2012): 044612. https://doi.org/10.1103/PhysRevC.86.044612
[28] Greiner, Walter, and Raj K. Gupta, eds. *Heavy elements and related new phenomena*. Vol. 1. World Scientific, 1999. https://doi.org/10.1142/3664
[29] Delion, D. S. "Universal decay rule for reduced widths." *Physical Review C* 80, no. 2 (2009): 024310. https://doi.org/10.1103/PhysRevC.80.024310
[30] Ismail, M., and A. Adel. "Effect of deformation parameters, Q value, and finite-range N N force on α-particle preformation probability." *Physical Review C* 89, no. 3 (2014): 034617. https://doi.org/10.1103/PhysRevC.89.034617
[31] Majekodunmi, Joshua T., M. Bhuyan, K. Anwar, N. Abdullah, and Raj Kumar. "Preformation Probability and Kinematics of Clusters Emission yielding Pb-daughters." *Chinese Physics C* 47, (2023): 074106. https://doi.org/10.1088/1674-1137/acbf2b
[32] Wang, Meng, G. Audi, F. G. Kondev, W. J. Huang, S. Naimi, and Xing Xu. "The AME2016 atomic mass evaluation." *Chin. Phys. C* 41, no. 030003 (2017): 1674-1137. https://doi.org/10.1088/1674-1137/41/3/030003
[33] Seif, W. M., and Laila H. Amer. "Systematic investigation of cluster radioactivity for uranium isotopes." *Nuclear Physics A* 969 (2018): 254-268. https://doi.org/10.1016/j.nuclphysa.2017.10.004
[34] Qi, Chong, F. R. Xu, Roberto J. Liotta, Ramon Wyss, M. Y. Zhang, C. Asawatangtrakuldee, and D. Hu. "Microscopic mechanism of charged-particle radioactivity and generalization of the Geiger-Nuttall law." *Physical Review C* 80, no. 4 (2009): 044326. https://doi.org/10.1103/PhysRevC.80.044326
[35] Warda, M., A. Zdeb, and Luis M. Robledo. "Cluster radioactivity in superheavy nuclei." *Physical Review C* 98, no. 4 (2018): 041602. https://doi.org/10.1103/PhysRevC.98.041602